The environment of high-redshift AGN

OLIMPIA JUDIT FOGASY

Department of Earth and Space Sciences
CHALMERS UNIVERSITY OF TECHNOLOGY
Gothenburg, Sweden 2016

The environment of high-redshift AGN
OLIMPIA JUDIT FOGASY

Radio Astronomy & Astrophysics Group
Department of Earth and Space Sciences
Chalmers University of Technology
SE–412 96 Gothenburg, Sweden
Phone: +46 (0)31–772 1000

Contact information:
Judit Fogasy
Onsala Space Observatory
Chalmers University of Technology
SE–439 92 Onsala, Sweden

Phone: +46 (0)31–772 5543
Fax: +46 (0)31–772 5590
Email: `judit.fogasy@chalmers.se`

The environment of high-redshift AGN

OLIMPIA JUDIT FOGASY
Department of Earth and Space Sciences
Chalmers University of Technology

Abstract

In order to understand the formation and evolution of local massive galaxies and to reveal the processes that engineered the tight correlations found between their supermassive black hole (SMBH) mass and bulge mass or velocity dispersion, the study of powerful, high-redshift active galactic nuclei (AGN) and their environment is crucial. As powerful high-z AGN are massive galaxies themselves, they likely trace proto-clusters, where the progenitors of present-day massive galaxies reside. Observations of high-z quasars and radio galaxies suggest that these AGN live in overdense environment surrounded by star-forming Lyα-emitters and submillimeter galaxies. At smaller scales several high-z quasars and radio galaxies have gas-rich, star-forming companion galaxies, such as the subject of the appended paper, the system of SMM J04135+10277.

This system consists of a SCUBA discovered type-1 quasar and a gas-rich companion galaxy at ~ 5"(~ 40 kpc) distance from the AGN position. The case of SMM J04135+10277 is particularly interesting, since the companion galaxy is associated with one of the most massive molecular gas reservoirs found in the high-z Universe ($M_{\mathrm{H_2}} \sim 10^{11}\,\mathrm{M_\odot}$), while the quasar seems to be gas-poor.
In order to determine the properties of the companion galaxy, we construct and model its spectral energy distribution (SED). We find that the companion galaxy is a heavily dust-obscured ($A_{\mathrm{V}} \gtrsim 2.8$), star-forming galaxy, with a star formation rate of $\sim 1000\,\mathrm{M_\odot\,yr^{-1}}$.

To test the uniqueness of this system and investigate the expected frequency of such quasar–star-forming galaxy pairs, we use the cosmological, semi-analytic model, GALFORM. We take the outputs of the simulation at $z = 2.8$ to find quasar–companion pairs at different separations. We find that 22% of our simulated quasar sample have at least one companion galaxy in their < 100 kpc environment and 0.3% have bright, star-forming companions (SFR $> 100\,\mathrm{M_\odot\,yr^{-1}}$).

To make a direct comparison between the model predictions and the case of SMM J04135+10277, we focus on systems with an integrated SFR of $> 500\,\mathrm{M_\odot\,yr^{-1}}$ inside the aperture and compute their relative gas content and SFR. We find that in 67% of these systems the molecular gas masses of the quasars' host galaxies are lower compared to the integrated value of their companions at a distance of < 50 kpc and the star formation is dominated by the companion galaxies and not the quasars' hosts. This means that the case of SMM J04135+10277 is representative of highly star-forming quasar–companion galaxy systems at $z = 2.8$.

Research contributions

This thesis is based on the work contained in the following paper:

- J. Fogasy, K. K. Knudsen, C. D. P. Lagos, G. Drouart, V. Gonzalez-Perez:
  On the frequency of star-forming galaxies in the vicinity of powerful AGN: the case of SMM J04135+10277
  Astronomy & Astrophysics, preparing for resubmission (2016)

I also participated in the following paper not included in the thesis:

- S. Frey, Z. Paragi, O. J. Fogasy, L. I. Gurvits:
  The first estimate of radio jet proper motion at $z > 5$
  Monthly Notices of the Royal Astronomical Society, 446, 3, p.2921-2928

Acknowledgements

Contents

Chapter 1

Introduction

1.1 Galaxies in different colours

One of the greatest and most important discoveries in the field of astronomy was the realization, that the Milky Way is just one of billions of galaxies in the Universe. Since then, millions of galaxies have been observed, studied and categorized, which revealed that galaxies come in many different colours and sizes and they undergo cosmic evolution.

Studies of the Milky Way and nearby galaxies helped to reveal the basic building blocks of galaxies and understand the underlying physics that connects them. In the most general sense a galaxy is a gravitationally bound system of stars. The regions between stars contain gas and dust, jointly referred to as the interstellar medium (ISM). In addition to stars and the ISM, galaxies have two other components, which are more difficult to observe. Stellar kinematic observations and dynamical models revealed that our Galaxy harbours a supermassive black hole (SMBH, $M_{\mathrm{BH}} \sim 10^6 M_\odot$) in its center (e.g. Eckart & Genzel 1996; Ghez et al. 1998; Genzel et al. 2000). Extensive studies of galaxies found similar conclusions and today it is widely accepted that every massive galaxy contains a supermassive black hole (e.g. Kormendy & Richstone 1995; Richstone et al. 1998; Magorrian et al. 1998; Kormendy & Ho 2013). The last component and maybe the most important is dark matter. The existence of dark matter is predicted by the Standard Model of Cosmology and it accounts for $\sim 85\%$ of the total mass in the Universe. Although dark matter has not been observed directly, evidence for its existence comes from e.g observations of galaxy kinematics and dynamics (galaxy rotation curve and velocity dispersion measurements), gravitational mass measurements of galaxy clusters, gravitational lensing, fluctuations in the cosmic microwave background (CMB).

Observations of galaxies in the local Universe showed bimodality regarding the colours and morphology of galaxies. The two main classes of galaxies are spiral

galaxies (late type), which are blue and star-forming, and elliptical galaxies (early type), which are red and passive in terms of star formation. The different colour of spiral and elliptical galaxies indicate different stellar populations: spiral galaxies have very mixed stellar populations, containing both young, hot, therefore blue Population I stars and old Populations II stars, while ellipticals have mostly old, cooler stars, and therefore they appear red.

The shape of elliptical galaxies is ellipsoidal, with smooth brightness profiles. Based on the shape of their isophotes, they can be disky or boxy ellipticals. Boxy ellipticals represent the highest mass galaxies in the Universe and contain large amount of X-ray gas in their halo, while disky ellipticals tend to be smaller in size and lack the hot X-ray gas component.

Spiral galaxies have more structure, they contain a thin rotating disk, a central, dense region of stars called bulge and in some cases bars. Bulges can be divided into two groups: classical bulges are much rounder than their disks, their Sérsic indices are $n \geq 2$; pseudo-bulges have more disky-like morphology, their Sérsic indices are $n \leq 2$.

1.2 Cosmic evolution of galaxies

The bimodality of present day[1] galaxies may arise from different evolutionary paths. In order to investigate how they formed, grew and reached their current appearance, one has to look at the various ways a galaxy can grow.

According to the currently accepted cosmological model, the Λ Cold Dark Matter model (ΛCDM), structure formation started from primordial density fluctuations followed by gravitational collapse of dark matter, leading to the formation of dark matter haloes. As the virial equilibrium is reached in the halo, the collapse of dark matter stops. Haloes then grow hierarchically, via merging with other virialized haloes. The deep potential well of dark matter haloes causes the baryonic matter to infall, collapse, radiate away its binding energy and form smaller structures, such as stars and galaxies.
There are two possible ways to supply a galaxy with gas and grow its stellar mass: merger events and gas accretion from the intergalactic medium (IGM).

Depending on the mass ratio of the merging galaxies, we distinguish between major (ratio>1:3), minor (<1:10) and intermediate (1:3–1:10) merger events. If the merging galaxies are gas-rich, the merger event is dissipative and is often referred to as "wet merger". In case of merging of gas-poor galaxies, the merger is "dry" and dissipationless. In general, wet-mergers were dominant at high-z, while dry merger events are more frequent at lower redshifts.

---

[1]The age of the Universe is ~ 13.8 Gyr. Adopting WMAP7 cosmology with $H_0 = 70.4$ km s^{-1}Mpc^{-1}, $\Omega_{\mathrm{m}} = 0.272$ and $\Omega_\Lambda = 0.728$, at redshifts $z = 3$ and $z = 2$ the Universe is ~ 2.2 Gyr and ~ 3.4 Gyr old, respectively.

Major gas-rich mergers are proposed to be responsible for triggering starburst events, driving gas into the central regions of the galaxy and fuelling the SMBH, which then appears as an active galactic nucleus (AGN) (e.g. Sanders & Mirabel 1996; Hopkins et al. 2006, 2008). As the AGN becomes more powerful it influences its host galaxy through AGN feedback, in form of winds, powerful outflows, and radio jets which eventually quench the star formation. While the merger scenario is appealing, observations of high-z star-forming galaxies and AGN studies indicate that mergers are not the only and dominant way of galaxy growth and AGN triggering.

Galaxies can accrete gas from the IGM. Based on the early studies of galaxy formation, which assumed spherical symmetry, gas falling into the potential well of a dark matter halo is shock-heated to the virial temperature of the halo ($T_{vir} \sim 10^6$ K) and reaches pressure supported quasi-static equilibrium with dark matter. By radiating away its thermal energy the gas can cool in the inner regions of the halo and settle into a rotationally supported disk, where it can form stars (e.g. Rees & Ostriker 1977; Silk 1977; Fall & Efstathiou 1980; White & Frenk 1991).

In contrast to early models of galaxy formation, hydrodynamical numerical simulations, such as the Virgo Consortium Millenium Simulation and the Illustris Simulation, show different geometry than spherical: the large scale structure of the Universe contains filaments and sheets, separated by empty spaces, voids (e.g. Springel et al. 2005; Vogelsberger et al. 2014). Galaxies primarily form along the filaments, the most massive galaxies at the intersections of filaments. Despite the different geometry, a substantial fraction of the gas still gets shock-heated in the simulations. This accretion mode is called "hot mode" (Katz et al. 2003; Kereš et al. 2005).

However, simulations also revealed that a large fraction of the accreted gas is never shock-heated to T_{vir} but radiates its gravitational energy from $T \leq 10^5$ K. This mode of accretion is called "cold mode" (Katz et al. 2003; Kereš et al. 2005). Galaxies fed along filaments can grow through cold mode accretion as the gas density in the filaments is high, leading to short cooling times. Moreover, both accretion modes can coexist, especially at high-z, where dense, cold filaments may penetrate through the hot haloes of massive galaxies (Kereš et al. 2005; Dekel et al. 2009).

The mode of gas accretion also depends on the redshift and the halo mass. At higher redshifts ($z > 3$) the density of the gas is higher, the radiative cooling is more efficient, hence cold accretion is more dominant. On the other hand, higher mass haloes have higher virial temperatures and therefore longer cooling times and the gas is accreted in hot mode. Thus cold accretion dominates in less dense environment and hot mode accretion dominates in group and cluster environments at low redshift.

By distinguishing between accretion onto haloes and galaxies, the specific accretion rate of haloes increases with halo mass, while the accretion rate onto galaxies
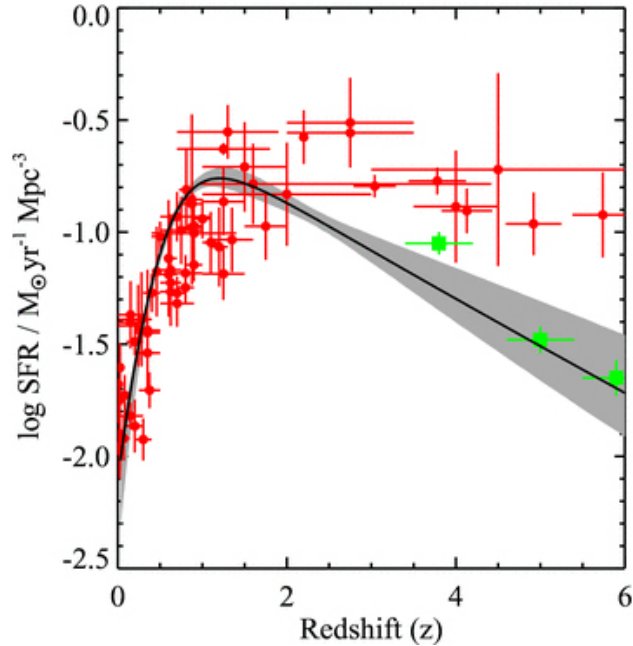
Figure 1.1: Redshift evolution of the black hole accretion rate (solid line; grey shaded area indicates 1σ uncertainty of the model) and the cosmic star formation rate (circles and squares from Hopkins 2004; Bouwens et al. 2007, respectively). The black hole accretion rate is scaled up by a factor of 5000. The figure is adapted from Aird et al. (2010, Fig.13).

drops at $M_{\rm halo} \gg 10^{12}\,{\rm M}_\odot$ (e.g. van de Voort et al. 2011b). Looking at the relative contribution of the two modes, the hot mode accreation onto haloes becomes more important at higher mass haloes ($M_{\rm halo} \geq 10^{11}\,{\rm M}_\odot$). However, the hot fraction of the gas accreted onto galaxies does not depend on the halo mass. Moreover, while the accretion onto haloes is insensitive to metal-line cooling and feedback from star formation and AGN, these processes affect the accretion onto galaxies, thus controlling their growth and evolution (e.g. van de Voort et al. 2011b).

Both merger events and gas accretion from the IGM play an important role in galaxy evolution: wet major mergers can induce vigorous starbursts and trigger luminous AGN, the most massive core-boxy ellipticals formed via dissipationless dry mergers, while cold accretion supplies disk galaxies and lower luminosity AGN. Moreover, the two modes of gas accretion gives a plausible explanation why massive systems are passive, while lower mass galaxies, spirals have on-going star formation.

Looking at the redshift evolution of the star formation rate density, it is clear that the Universe was much more active at higher-redshifts (Figure 1.1). The peak of the star formation rate density is around $z = 2 - 3$, which is followed by

an exponential decline toward lower redshifts. At the peak, the star formation rate (SFR) was $\sim 10\times$ higher compared to its present day value (e.g. Madau & Dickinson 2014). The evolution of the cosmic star formation rate is governed by the growth of dark matter haloes and the gas accretion mode. Based on numerical simulations, the decline of the global SFR might be the result of the drop of the global cold accretion mode onto haloes (e.g. van de Voort et al. 2011a). While the hot mode accretion does not show such drop, a large fraction of the accreted gas has longer cooling time than the Hubble time, thus it cannot be accreted by the galaxies to feed star formation.

1.3 High-redshift galaxies

Over the past decades several techniques have been developed to identify high-redshift galaxies, which is necessary in order to get an unbiased picture of high-z galaxy populations and their properties (e.g. stellar mass, star formation rate) and understand their formation and evolution. Based on different selection criteria we can trace different high-z galaxy populations, such as star-forming Lyman-break and *BzK* galaxies, extreme starburst galaxies like submillimeter galaxies (SMGs) or massive galaxies, like extremely red objects (EROs) and distant red galaxies (DRGs). Briefly, the most common characteristics of these high-redshift galaxies are:

Lyman-break galaxies:
The Lyman-break galaxies are selected by the Lyman-break technique, which enables us to detect these galaxies in the optical regime (e.g. Partridge & Peebles 1967; Steidel et al. 1995). As young stars emit mostly UV light and photons with energies higher than the ionization energy of hydrogen are easily absorbed by neutral gas around star-forming regions, a break can be observed in the spectral energy distribution (SED) of the galaxy at $91.2\,\mathrm{nm}$ rest-frame wavelength. In case of high-z galaxies ($z \gtrsim 2.5$) this break will be redshifted to the optical band, thus can be used as tracers of star-forming, distant galaxies.

***BzK* galaxies:**
The *BzK* criteria selects both star-forming and passively evolving galaxies at redshifts of $1.4 < z < 2.5$ based on two-colour criteria using the B, z and K photometric bands (Daddi et al. 2004). *BzK* galaxies can be identified by the following criteria:

$$BzK = (z - K)_{\mathrm{AB}} - (B - z)_{\mathrm{AB}}$$

where $BzK \geq -0.2$ selects star-forming and $BzK < -0.2 \cap (z - K)_{\mathrm{AB}} > 2.5$ selects passive galaxies at $z > 1.4$. Compared to UV selected galaxies at $z \sim 2$, *BzK* galaxies have higher reddening and star formation rate. Their redshift distribution and mass is similar to that of SMGs but the later have higher SFR, while *BzK* galaxies have higher space density.

Distant red galaxies and extremly red objects:
In case of very red galaxies, either because of dust reddening or containing old stellar populations, near-infrared imaging can be used to select high-z galaxies via the rest-frame Balmer-break and the 400 nm-break, which is due to metal line absorption in the atmospheres of old stars. DRG can be identified at redshifts $2 < z < 4$ using the J and K band with the following criteria in the Vega photometric system: $J - K > 2.3$ (e.g. Franx et al. 2003).

Extremely red objects are also selected according to their very red optical to near-infrared colours and represent both star-forming systems and old passively evolving galaxies. EROs are mostly lower redshift sources ($z \sim 1$). The selection criteria is based on R and B bands: $R - K \gtrsim 5$ (Elston et al. 1988).

Submillimeter galaxies:
Submillimeter galaxies are heavily dust-obscured high-redshift ($z \gtrsim 2$) starburst galaxies (SFR $\gtrsim 1000 \, \mathrm{M_\odot \, yr^{-1}}$). SMGs are often faint in the UV-optical bands but bright at submillimeter/mm wavelengths due to the thermal emission produced by dust grains (e.g. Blain et al. 2002). The dust emission is well-described by a modified blackbody spectrum with a peak close to $100 \, \mu\mathrm{m}$. The advantge of submm observations is the large negative K-correction as they sample the Rayleigh-Jeans regime of the SED, which is a strongly increasing function of the frequency. Thus high-z galaxies have very similar brightness at submm wavelengths from $z = 1 - 8$ (e.g. Casey et al. 2014).

1.4   Coevolution of SMBHs and Their Host Galaxies

General references: Kormendy & Ho (2013)
Observations of local, massive elliptical galaxies found tight correlations between the mass (M_bulge) or velocity dispersion (σ) of the host galaxy and the mass of its supermassive black hole (M_BH) (e.g. Magorrian et al. 1998; Gebhardt et al. 2000; Merritt & Ferrarese 2001; Marconi & Hunt 2003). Equation 1.1 shows the above correlations for ellipticals and classical bulges:

$$\frac{M_\mathrm{BH}}{10^9 \mathrm{M_\odot}} = 0.542^{+0.069}_{-0.061} \left(\frac{L_\mathrm{K,bulge}}{10^{11} \mathrm{L_{K\odot}}} \right)^{1.21 \pm 0.09},$$

$$\frac{M_\mathrm{BH}}{10^9 \mathrm{M_\odot}} = 0.309^{+0.037}_{-0.033} \left(\frac{\sigma}{200 \mathrm{km s^{-1}}} \right)^{4.38 \pm 0.29}, \tag{1.1}$$

$$\frac{M_\mathrm{BH}}{10^9 \mathrm{M_\odot}} = 0.49^{+0.06}_{-0.05} \left(\frac{M_\mathrm{bulge}}{10^{11} \mathrm{M_\odot}} \right)^{1.16 \pm 0.08},$$

based on the compilation of extensive samples (Kormendy & Ho 2013).

An interesting aspect of these correlations, that they only hold for elliptical galaxies and galaxies with classical bulges. The M_BH does not correlate with so

called pseudo-bulges or disk galaxies, nor with galaxy disks. This suggests that SMBHs in disk galaxies and classical bulges/ellipticals might grow via different feeding mechanisms. During major galaxy mergers all conditions are met so that global feeding can occur, which likely leads to the formation of classical bulges and ellipticals. On the other hand, SMBHs in disk galaxies are fed via secular, internal processes which cannot engineer a tight correlation between the SMBHs and their host galaxies.

Besides the tight correlations between $M_{\mathrm{BH}} - M_{\mathrm{bulge}}$ and $M_{\mathrm{BH}} - \sigma$, there are other signs suggesting that SMBHs and ellipticals/bulges evolve together. For example, the histories of the cosmic star formation rate and black hole growth are similiar (Figure 1.1), a significant fraction of starburst galaxies contain burried AGN and the host galaxies of luminous AGN tend to be star-forming. This implies that AGN activity and star formation is linked. Based on the Soltan's argument, most of the SMBH mass must have been grown while the galaxy hosted an AGN, which means that SMBHs in local galaxies are the final products of high-redshift AGN episodes. Thus, beyond major merger events, AGN feedback may play an important role in establishing the observed correlations.

1.5 The aim of this thesis

How do galaxies grow and evolve? What is the origin of the local bimodal distribution of galaxies regarding their colour, morphology, star formation? What processes engineer the tight correlations found between the SMBH mass and the bulge mass/velocity dispersion of local massive galaxies? When are these correlations established? How does the host galaxy know what happens near the SMBH and vice versa? What are the processes that trigger the growth of the SMBH and star formation in the host? Where and how did the stellar mass of local massive ellipticals form and assemble: during starburst events triggered by galaxy interactions, by mergers of gas-rich progenitors or in close star-forming companion galaxies of high-redshift AGN, which eventually merged? What role does the environment play in galaxy formation?

These questions have inspired many scientists in the last twenty years and though a significant amount of progress has been made, many of the fundamental questions still lack answers. One way to start is to study high-z luminous AGN and their environment. As powerful AGN are massive galaxies themselves, they likely trace overdense environments or proto-clusters, where the progenitors of present day massive ellipticals reside. Moreover, AGN are valuable and interesting targets, since their SMBHs are feeding and growing, which opens the opportunity to unfold how the growth of the black hole influences the growth of its host galaxy.

The aim of this thesis is to study the environment of high-z quasars and radio galaxies, the possible progenitors of local massive galaxies. Section 2 gives a summary of the current AGN classification scheme and unification theory and

discusses the role of AGN feedback in the evolution of massive galaxies. Section 3 summarises the results of recent AGN environment studies both on large and small scales. Section 4 gives an introduction to the appended paper and summarises its results. Section 5 gives an outlook and discusses future prospects.

Chapter 2

Active Galactic Nuclei

Active galactic nuclei (AGN) are the most powerful objects in the Universe, they release enormous amount of energy ($10^{42} - 10^{47}$ erg s^{-1}) over a wide range of the electromagnetic spectrum, from the X-ray and UV band till the infrared and radio bands. AGN are compact regions in the centre of galaxies, referred to as active galaxies. The central engines that power AGN are accreting supermassive black holes with a black hole mass between $10^6 - 10^9$ M$_\odot$.

The term active galactic nuclei represents a very broad and diverse group of extragalactic sources, which have considerably different properties and emission features. Therefore the classification and unification of AGN is an important step in order to reveal and understand the main physical processes involved in the triggering and fuelling of these sources. The study of AGN is also important in terms of galaxy evolution, as AGN can have a significant impact on their surroundings through feedback processes.

2.1 Classification of AGN

General references: Urry & Padovani (1995), Tadhunter (2008)
The classification of AGN is a complex method based on several critiria, e.g. energetics, optical and UV spectral features, optical and radio morphology, spectral shape, luminosity and variability. The most commonly used classification method divides AGN into three main groups basen on their optical and UV spectra, called *Type 1*, *Type 2* and *Type 0*. These groups can be divided into several subgroups based on radio luminosity and nuclear luminosity. Another way to classify AGN is to look at their energetics and the main form of their energy output.

2.1.1   Classification based on optical and ultraviolet spectra

Type 1 AGN

The spectra of Type 1 AGN have bright continua and contain broad (typically $1000 - 2000$ km s^{-1}) permitted and semiforbidden emission lines from hot, high velocity gas. In addition to the broad emission lines, most Type 1 AGN show strong, high-ionization narrow emission lines. The group of radio-quiet Type 1 AGN contains Seyfert 1 galaxies and radio-quiet quasi-stellar objects (QSO). Seyfert 1 galaxies are relatively low luminosity, lower redshift spiral galaxies, their host galaxies can be often resolved. On the contrary, QSOs are much more luminous which makes the observation of their host galaxies impossible in the optical regime. The radio-loud subgroup of Type 1 AGN consists of the low luminosity broad line radio galaxies (BLRG) and high luminosity radio-loud quasars (RLQ), which can be further divided depending on the shape of their radio spectra: steep radio spectrum dominated or flat radio spectra dominated RLQs.

Type 2 AGN

Type 2 AGN show only strong narrow emission lines and apparently no broad emission lines. Such sources are Seyfert 2 galaxies and narrow line X-ray galaxies in the radio-quiet subgroup and narrow line radio galaxies in the radio-loud subgroup. Some of these AGN are actually Type 1 sources but the broad emission lines are hidden and can be only seen in polarized light. On the other hand, there are sources refered to as "real" Type 2 AGN, which do not have any detectable broad lines. These AGN have lower luminosities compared to Type 2 sources with hidden broad emission lines.

Type 0 AGN

A small fraction of radio-loud AGN are collectively called 'blazars'. These AGN are highly variable sources, with their relativistic jets oriented close to the line-of-sight. Some of these AGN have no strong emission and absorption features in their spectra, such as BL Lacertae (BL Lac) objects. Optically violently variable (OVV) quasars have similar continua to BL Lac objects but their optical/UV spectra has a feature called "Big Blue Bump" inspite of their strong synchrotron radiation.

2.1.2   Radiative-mode and jet-mode AGN

General references: Heckman & Best (2014)

Heckman & Best (2014) presented strong empirical evidence that the local AGN population can be divided into two major groups based on their energetics, by deriving their Eddington ratio, which is the ratio of AGN bolometric luminosity and the Eddington luminosity. The Eddington luminosity sets an upper limit to the luminosity of a spherically accreting object with a given mass (M):

$$L_{Edd} = \frac{4\pi G m_{\mathrm{p}} c}{\sigma_T} M_{\mathrm{BH}} = 1.5 \times 10^{38} \frac{M_{\mathrm{BH}}}{M_\odot} \ \mathrm{erg \, s^{-1}} \qquad (2.1)$$

where m_p is the mass of a proton, c is the speed of light and σ_T is the Thompson cross-section for electron scattering (Netzer 2015). Above this luminosity the object is not in equilibrium anymore, the radiation pressure exceeds the gravitational force and the gas will be blown away by the radiation. AGN with high Eddington ratio ($\mathrm{L_{bol}}/\mathrm{L_{Edd}} \gtrsim 0.01$) are called radiative mode AGN or high-ionization AGN. Their main energy output is in the form of electromagnetic radiation, which is produced by effective gas accretion through an optically thick accretion disk. Approximately 10% of these source are radio-loud. AGN with lower Eddington ratio ($\mathrm{L_{bol}}/\mathrm{L_{Edd}} \lesssim 0.01$) are jet-mode or low-ionization AGN and the main energy output is through kinetic energy transported by jets, powered by radiatively inefficient accretion flows (RIAF) or advection dominated accretion flows (ADAF).

Both radiative mode and jet-mode AGN are found over the full range of radio powers but a characteristic switch happens around $P_{4.1\,\mathrm{GHz}} \sim 10^{25}\,\mathrm{W\,Hz^{-1}}$. Above this radio power, radio sources are mostly radiative mode AGN, below this value the majority of radio-loud AGN are jet-mode. At higher redshift ($z > 1$) radiative mode AGN dominate at all radio luminosities, while in the local Universe jet-mode AGN dominate the radio population except the highest radio luminosity sources. Regarding their host galaxies, radiative mode radio-loud AGN are associated with on-going star formation in their hosts, while the host galaxies of jet-mode AGN are red and passive.

Radiative and jet mode AGN can be further divided into subgroups based on their emission spectra and radio-power:

- Radiative mode Type 1 AGN have both broad permitted and narrow emission lines in their spectra and can be radio-loud quasars or radio-quiet QSOs and Seyfert 1 galaxies

- Radiative mode Type 2 AGN have only strong narrow emission lines in their spectra and can be high-excitation radio sources or radio-quiet QSOs and Seyfert 2 galaxies

- Jet-mode AGN have weak to moderate strength narrow, low-ionization emission lines and can be low-excitation radio sources or LINERS (galaxies with low-ionization nuclear emission line regions)

2.1.3 Fanaroff-Riley classification

Radio-loud AGN can be classified on the basis of their extended radio structures (Fanaroff & Riley 1974). Fanaroff-Riley I (FRI) radio galaxies have bright inner jets but they flare and their intensity gradually decreases from the nucleus, while FRII radio galaxies have highly collimated jets, ending in prominent radio lobes and hot spots. FRII radio sources are generally more powerful, hence they are more efficient in transporting energy toward their lobes. In case of FRII radio sources the relativistic jets can maintain their energy as they propagate through
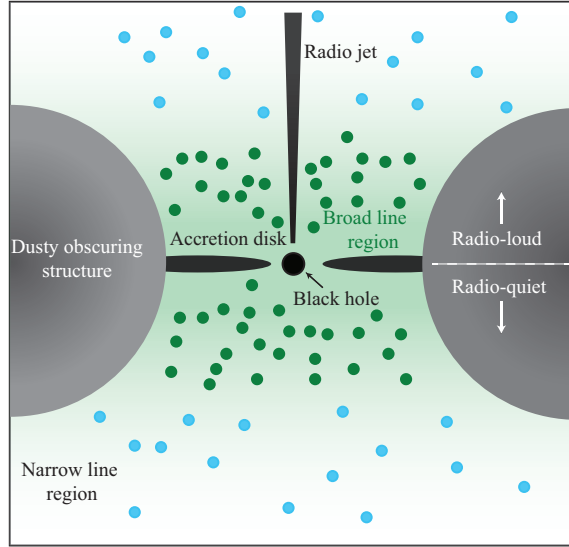
Figure 2.1: The schematic view of the central region of radiative-mode AGN based on Heckman & Best (2014).

the host galaxy, while the jets of FRI sources dissipate their energy due to the interaction with the surrounding medium.

The switch between FR I and FR II morphology is around $P_{4.1\,\mathrm{GHz}} \sim 10^{25}\,\mathrm{W\,Hz^{-1}}$. While there is an overlap between radiative mode AGN and radio sources with FR II morphology, as well as between jet-mode AGN and FR I radio sources, this is due to the similar radio power at which the switch occurs between these AGN populations and does not mean that the radio morphology and the nature of the accretion flow depend on each other. Both radiative-mode FR I and jet-mode FR II radio sources exist.

2.2   The Unified Model of AGN

General references: Antonucci (1993); Urry & Padovani (1995); Tadhunter (2008) The Unified Model of AGN proposes the idea that the only difference between Type1/Type 2 AGN or radio-loud/radio-quiet AGN is in their orientation relative to the observer's line-of-sight. The unification of AGN has two important pillars, the effect of relativistic beaming and anisotropic obscuration by an optically thick region surrounded the AGN. Relativistic beaming means that the apparent luminosity of the AGN seems higher if the radio jet is pointing closer to line-of-sight.

Figure 2.1 illustrates the schematic structure of the central part of AGN. In case of radiative mode AGN, the SMBH is fed by gas inflow from a geometrically thin, optically thick accretion disk. The accretion disk is surrounded by a hot corona, where photons are Compton-scattered up to X-ray energy levels. Both

the accretion disk and the hot corona emit highly ionizing radiation, which photoionizes any dense clouds close to the nucleus. This region of high velocity gas ($\sim 1000\,\mathrm{km\,s^{-1}}$) associated with UV-to-near-IR permitted emission lines is called the Broad Line Region.

On larger scale, the accretion disk and the SMBH are surrounded by an obscuring, clumpy structure (often referred to as torus), which consists of dust and molecular gas ($N \sim 10^{23} - 10^{25}\,\mathrm{cm^{-2}}$). This obscuring structure is responsible for the thermal IR emission of AGN. In some cases the opacity of the torus is so high, that even the hardest X-ray photons cannot escape from it (Compton-thick). The only exit for the ionizing radiation coming from the accretion disk and corona is along the polar axis of the torus. These escaping photons photoionize gas clouds at higher distances from the SMBH. This region of lower density and lower velocity gas at a scale of $0.1 - 1\,\mathrm{kpc}$ is called the Narrow Line Region, from where the UV-to-IR forbidden and permitted narrow ($\sim 100\,\mathrm{km\,s^{-1}}$) emission lines originate.

Based on the above picture the unification scheme easily emerges. If the observer's line-of-sight is close to the polar axis of the torus, the AGN can be seen directly: in case of Type 1 AGN the SMBH, the accretion disk and the Broad Line Region is not obscured, therefore their observed spectra contain both narrow and broad emission lines. If the viewing angle of the AGN is closer to the equatorial axis of the obscuring torus, the AGN is obscured. The spectra of these obscured, Type 2 AGN only contain narrow emission lines, since the Broad Line Region is hidden.

In case of radio-loud AGN the combination of the orientation effects and the relativistic beaming is necessary to explain the observed differences between radio-loud quasars and radio galaxies, such as the lack of broad permitted lines and Big Blue Bump continuum emission in radio galaxies (Barthel 1989). When the radio jet is oriented in a large angle relative to the line-of-sight, the central part of the AGN is hidden by the dusty circumnuclear torus and the object can be observed as a narrow line radio galaxies. If the radio jet is pointing closer to the line-of-sight, the central AGN is becomes visible and the AGN is classified as a quasar, with steep radio spectrum. At a very small angle between the radio jet and the line-of-sight, the relativistic jets are beamed and the AGN is dominated by the flat radio spectrum and is observed as a higly variable, blasar or an OVV quasar.

2.3 The role of AGN-feedback

General references: Fabian (2012); Heckman & Best (2014)
AGN feedback is the interaction of the central SMBH and its host galaxy through the energy and radiation generated by the accreting SMBH. As the binding energy of an accreting SMBH is significantly larger than that of the bulge, the feedback from the AGN must have a great impact on its host galaxy. AGN feedback has two distinct modes based on the nature of the energy outflows near the SMBH,

radiative mode (quasar or wind mode) and kinetic mode (radio-jet or maintenance mode).

The radiative mode AGN feedback requires radiatively efficient accretion flow, thus it occurs in sources with high Eddington ratio: in case of luminous quasars/AGN and generally in the early, young stages of these sources. This feedback mode was probably most effective at the peak of quasar activity ($z \sim 2 - 3$), when galaxies were more gas-rich. Radiative mode feedback can act in form of radiation pressure on the surrounding medium, specifically on dust grains or in form of AGN winds and outflows.

In case of radiation pressure driven feedback, the UV emission radiated by the AGN is easily absorbed by dust grains, which reradiate them in the IR regime. If the surrounding gas is optically thick, these IR photons can undergo multiple scattering while momentum flux is transferred to them. As a result radiation pressure can drive a shell of dusty gas into the host galaxy. However, this radiation-powered flow can only move outward until the medium is optically thick.

Interaction may occur through high velocity winds, observed as line absorption in the AGN continuum or galactic scale outflows, with outflow rates of hundreds to thousands $M_\odot \, yr^{-1}$ and velocities up to thounsands of $km \, s^{-1}$ (e.g. Walter et al. 2002; Prochaska & Hennawi 2009; Morganti et al. 2007; Feruglio et al. 2010; Nesvadba et al. 2011; Aalto et al. 2012; Greene et al. 2012; Rupke & Veilleux 2013). Given the high velocities and outflow rates, radiative mode AGN feedback is the only plausible explanation to their origin. Such outflows are able to expel the gas from the host galaxy and quench star formation, thus regulating the growth of both the SMBH and the host galaxy: the galaxy is moving from the blue, star-forming sequence to the red sequence of galaxies. Thus radiative mode feedback may be responsible for setting up the observed correlations between black hole mass and bulge properties.

Kinetic mode feedback operates in lower redshift, massive, "red and dead" galaxies, typically living in the centers of galaxy groups and clusters. However, they are surrounded by X-ray emitting gas with cooling times in the central regions of the clusters shorter than the Hubble time, which would result in cooling flows with cooling rates of thousands of $M_\odot \, yr^{-1}$ in the absence of feedback mechanisms. This huge amount of gas would boost the star formation and the stellar mass of the galaxy would significantly grow. But something acts against the cooling: maintenance mode AGN feedback. According to the general consensus, as the cooling of the gas begins in the central regions and reaches the SMBH it will generate powerful jets, which inject energy back to the halo and the intracluster medium by inflating bubbles of relativistic plasma in order to balance the energy loss by radiative cooling. Such bubbles or cavities are clearly seen in X-ray and radio observations (e.g. Boehringer et al. 1993; McNamara et al. 2000; Dunn & Fabian 2006, 2008). Hence this feedback maintains the "red and dead" state of the galaxy and the correlation between the SMBH and the bulge of its host galaxy.

Chapter 3

The environment of high-z AGN

In order to gain insight into the formation and evolution of local massive, so-called "red and dead", elliptical galaxies one has to look back in time to find and study their progenitors. Since merger events played an important role in building these massive galaxies, proto-clusters might be the scene of these events. Proto-clusters are overdense structures of galaxies at high redshift ($z > 2$), which are still forming and are not bound and virialised systems. The proto-cluster members, the progenitors of local massive ellipticals, are gas-rich and star-forming galaxies. As the most luminous high-z AGN are massive galaxies themselves, they likely live in overdense environment and can be used as tracers of proto-clusters and dense regions. High-z radio galaxies (HzRGs) and quasars are among the favoured targets for such studies.

Indeed, recent studies of high-z powerful AGN found such overdensities of star-forming galaxies in their environment both at large and small scales using observational probes such as Lyα and Hα emission lines, mid-IR emission from stars or dust emission in submm and mm bands. For example, narrow band imaging of the radio galaxy MRC 1138–262 ($z = 2.16$) found ~ 50 Lyα emitting galaxies (LAEs) in its $8.3\,\mathrm{Mpc}^2$ field and subsequent spectroscopic observations confirmed that 15 of these sources are at the same redshift as the HzRG (Kurk et al. 2000, 2004b; Pentericci et al. 2000; Croft et al. 2005). Hα emission line studies of the field of MRC 1138–262 also showed overdensities of star-forming galaxies towards the radio galaxy (Kurk et al. 2004b,a). Moreover, Venemans et al. (2007) studied the $9\,\mathrm{Mpc}^2$ field of eight radio galaxies ($z = 2.1 - 4.1$) and searched for LAEs in their fields. In case of six fields they found a factor of $3 - 5$ overdensity of LAEs compared to the volume density of field Lyα emitters at similar redshifts.

Deep submm observations and mid-IR studies of luminous AGN led to similar conclusions. Stevens et al. (2003) used the Submillimetre Common-User Bolometer Array (SCUBA) on the James Clerk Maxwell Telescope (JCMT) to study seven HzRGs and found an overdensity of submm sources around their targets. A

surprising feature of their findings is the observed alignments of the radio axis of HzRGs with their brightest submm sources, indicating that they trace the large-scale structure around the HzRGs. An excess of star-forming galaxies have been also discovered in case of X-ray and optically selected high-z quasars (Stevens et al. 2004; Priddey et al. 2008; Stevens et al. 2010).

The CARLA program (Clusters Around Radio-Loud AGN) used the Infrared Array Camera (IRAC) on board of *Spitzer Space Telescope* to investigate the environment of a large sample of radio loud quasars and HzRGs at $1.2 < z < 3.2$ (Wylezalek et al. 2013). During this program the field of 387 radio-loud AGN have been observed in the $3.6\,\mu m$ and $4.5\,\mu m$ IRAC bands. To identify high-z sources in the field of the AGN, the potential galaxy cluster members, they used the colour cut $[3.6] - [4.5] > -0.1\,(\mathrm{AB})$, which selects galaxies above $z > 1.3$. They found that $\sim 55\%$ of the radio-loud AGN fields are overdense at 2σ level and $\sim 10\%$ are overdense at 5σ level compared to sources selected similarly in blank fields. An interesting aspect of their results is that they did not find any sign of dependence of environment on radio luminosity and the fields of radio-loud quasars and HzRGs are quite similar.

In addition, submm observations of WISE (Wide-field Infrared Survey Explorer) and radio-selected, luminous AGN discovered a factor of $4 - 6$ overdensity of submm galaxies in their 1.5 arcmin-radius environment compared to blank-field surveys, suggesting that WISE/radio selected AGN are signposts of overdense regions of dusty, star-forming galaxies (Jones et al. 2015). Silva et al. (2015) found even higher excess of SMGs around WISE/radio selected hyper-luminous quasars ($z \sim 2$) using ALMA (Atacama Large Millimetre Array) at a scale of $150\,\mathrm{kpc}$.

At smaller scales, gas-rich, star-forming companion galaxies have been discovered for a number of high-z quasars and radio galaxies, in some cases these systems are alreay in the early/late stage of a merger event (e.g. Ivison et al. 2000; De Breuck et al. 2005; Greve et al. 2007; Ivison et al. 2008; Riechers et al. 2008; Nesvadba et al. 2009; Clements et al. 2009; Ivison et al. 2012; Salomé et al. 2012; Riechers 2013; Husband et al. 2015; Gullberg et al. 2016)

One of the many interesting sources is the quasar BR1202-0725 ($z = 4.7$), which has a starburst companion at $\sim 25\,\mathrm{kpc}$ distance, while high-resolution ALMA observations discovered that both of these objects have even closer companion galaxies, indicating that this complex system is in a gas-rich, multiple merger event (Salomé et al. 2012). Another fascinating example is the quasar PKS1614+051 ($z = 3.2$), which has four Lyα-emitting companion galaxies, from which three are in the close vicinity of the quasar, suggesting that they eventually merge into a massive galaxy by $z \sim 1$ (Husband et al. 2015).

While the host galaxies of high-z AGN in the above systems are gas-rich and/or star-forming themselves, there are several AGN–companion galaxy systems, in which most of the star formation is not happening in the host galaxies of the AGN but rather in the companion galaxies. For instance, Clements et al. (2009)

discovered extended submm emission offset from the quasar SDSS 160705+533558 ($z = 3.65$) and concluded that this object is an early stage of a merger event between the gas-poor host galaxy of the AGN and a gas-rich, starburst galaxy. The case of SMM J04135+10277 ($z = 2.8$) is very similar: while this quasar was discovered through its bright submm emission (Knudsen et al. 2003) and previous CO observations detected large amount of gas ($M_{\mathrm{H_2}} \sim 10^{11}\,\mathrm{M_\odot}$), recent CO(3-2) observations revealed that this massive gas reservoirs is associated with an optically faint, gas-rich companion galaxy and not the quasar (Riechers 2013). If these systems undergo a merger event and build a massive elliptical by $z \sim 0$, then a significant fraction of the stellar mass of the forming elliptical galaxy was built up in the companion, while the SMBH of the forming elliptical grew in the host galaxy of the AGN. However, if this is the case, how is the well-known $M_{\mathrm{BH}} - M_{\mathrm{bulge}}$ correlation established? It might be that the SMBH also grows significantly during the merger through gas accretion supplied by the companaion galaxy or through merger averaging, if the companion galaxy also harbours a SMBH.

The observed richness of star-forming, gas-rich galaxies in the environment of HzRGs and quasars demonstrate the relevance of such studies in finding the progenitors of massive local galaxies and the discovery of close high-z AGN–star-forming companion galaxy pairs and early/late mergers highlights the importance of high resolution observations in order to understand their formation. One way to proceed is to study FIR-bright quasars with high resolution.

Chapter 4

Introduction to the appended paper

In the appended paper we study the system of SMM J04135+10277 ($z = 2.84$), which consists of a SCUBA discovered type-1 quasar (Knudsen et al. 2003) and a gas-rich companion galaxy at $\sim 5"(\sim 40\,\mathrm{kpc})$ distance from the AGN position. This system is particularly interesting, since the companion galaxy is associated with one of the most massive molecular gas reservoirs found in the high-z Universe ($M_{\mathrm{H_2}} \sim 10^{11}\,\mathrm{M_\odot}$), while the quasar seems to be gas-poor (Riechers 2013). In order to investigate the properties of the companion galaxy, we construct and model its spectral energy distribution (SED). With the aim of investigating the expected frequency of such systems in a cosmological setup, we use a cosmological, semi-analytical model. My contribution to the appended paper includes the photometry of the companion galaxy, modelling its spectral energy distribution, actively participating in the preparation of the simulation and in the interpretation of its results, and writing the manuscript. Below I give a brief introduction to SED modelling and semi-analytical modelling of galaxy formation and evolution.

4.1 SED modelling

General references: Conroy (2013)
The spectral energy distribution shows the energy output of a galaxy over the electromagnetic spectrum (Figure 4.1). As galaxies have many different building blocks (old and young stars, gas, dust, AGN etc.), each of these components influence the final shape of the SED. Old stars are cooler, thus they emit their energy in the red end of the optical band and in the near-IR, while hot, young stars are bright in the blue part of the optical band and in UV. Dust is an important tracer of star formation and hidden AGN, as it absorbs the UV and optical light and reemits it in the infrared. If the galaxy harbours an AGN, it can have a significant contribution to the final galaxy SED in the X-ray, UV, optical, IR and radio bands. Two important SED features that indicate the presence of an AGN

are the "Big Blue Bump", which is related to thermal emission from the accretion disk and the IR bump, which originates from thermal emission from dust at a wide range of temperatures. Since the SED of galaxies contain fundamental information about their stellar populations, star-formation history, gas and dust content and their overall evolution, disentengling the observed SEDs is of great importance. SED modelling is a powerful tool to extract information from the observed SEDs. Stellar population synthesis (SPS) models are widely used and have become very popular.

The first ingredient of SPS models is a simple stellar population (SSP), which represents the time evolution of a single population of coeval stars with a given metallicity and abundance pattern. To construct the SSP one has to combine stellar evolution theory in form of isochrones, stellar spectral libraries and the initial mass function (IMF). An isochrone specifies the location of stars with the same age and metallicity on the Hertzsprung-Russel diagram and are constructed from stellar evolution calculations. Stellar spectral libraries contain a large set of stellar spectra with different metallicity, effective temperature and luminosity and can be constrained from empirical studies or purely theoretical models. The IMF describes the initial stellar mass distribution of a stellar population entering the main sequence on the Hertzsprung-Russel diagram. The initial mass is a very important parameter of stars, since it determines their lifetime, luminosity and the chemical enrichment of the ISM. The most popular IMF models are the Salpeter, Kroupa, and Chabrier (Salpeter 1955; Kroupa 2002; Chabrier 2003) models. The next step of SPS models is to construct composite stellar populations by combing simple stellar populations with different ages and metallicities with the effect of dust (attenuation and emission). The effect of nebular emission on the SED also needs to be taken account as its contribution to the broadband fluxes can be high, thus it can have a significant impact on the derived parameters.

By modelling the SED, several important parameters can be derived, such as the stellar mass, star formation rate, star-formation history, metallicity, dust attenuation. Moreover, in case of high-z studies, the SED can be used to determine photometric redshifts, if spectroscopic redshifts are not available. The infrared emission of dust grains provides additional information about the physical properties of a galaxy, including dust luminosity, dust temperature and dust mass. The dust temperature of star-forming galaxies is typically $\sim 30 - 60\,\mathrm{K}$, while AGN have higher dust temperature ($T_{\mathrm{dust}} \gtrsim 60 - 100\,\mathrm{K}$).

In the appended paper we present SED modelling using the starburst SED model of Groves et al. (2008)[1] and the MAGPHYS code with high-z extensions[2] (da Cunha et al. 2008, 2015). The theoretical model of Groves et al. (2008) combines the spectral synthesis code of Starburst99 (Leitherer et al. 1999), the photoionization code MAPPINGS III and a dynamical evolution model of HII regions. The

---

[1]Publicly available at `http://www.mpia.de/~brent`.
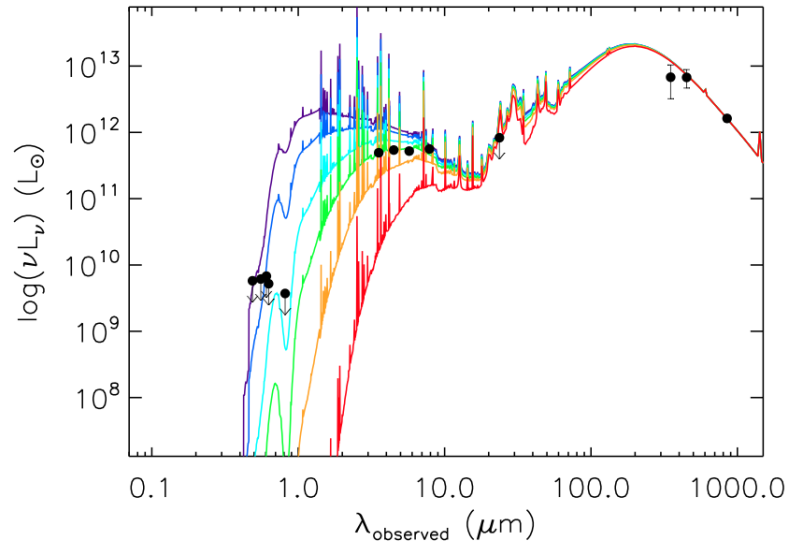[2]Publicly available at `http://www.iap.fr/magphys`.

Figure 4.1: The spectral energy distribution of the companion galaxy of SMM J04135+10277. The curves demonstrate how the model SED changes for different visual extinction values ($A_\mathrm{V} = 0.8, 1.3, 2.3, 3.3, 5.3, 11.3$ mag) from top to bottom. The best-fit Groves et al. (2008) model has $A_\mathrm{V} = 3.3$ mag.

novelty of this model is that instead of treating the starburst as a single spherical radiation transfer problem, this model splits up the starburst into many individual HII regions and the global SED is the sum of the SEDs of these HII regions and their surrounding photodissociation regions (PDR). The main components to construct a model SED from the model library are templates of HII regions surrounding young stellar clusters, PDRs, young ultra compact HII regions, old stellar populations and diffuse dust emission. The dust attenuation of stellar light is produced by a foreground dusty screen (Fischera & Dopita 2004, 2005). The models also include the effect of varying metallicity.

The MAGPHYS code is one of the commonly used SED fitting codes (e.g. Lanz et al. 2013; Rowlands et al. 2014; Smolčić et al. 2015). MAGPHYS models the star formation history, dust attenuation and metallicity of galaxies and combines the stellar emission with dust emission using energy balance technique. To compare the model SED with the observed, a Bayesian approach is used. The optical model library of the code is derived using the Bruzual & Charlot (2003) population synthesis code and the attenuation by dust is included via the two-component model of Charlot & Fall (2000). The infrared model library is computed by combining the infrared emission from stellar birth clouds and the ambient ISM. The main advantage of the MAGPHYS code is the consistent modelling of the ultraviolet-to-infared spectral energy distribution of galaxies. However, in contrast to the Groves et al. (2008), it is not possible to control or fix the fitting parameters.

4.2   Semi-analytical modelling of galaxy formation

While the evolution of dark matter haloes in the ΛCDM model is well understood, the evolution of the baryonic component is more complex, since it involves many processes, which also interact and influence each other (e.g. star formation, feedback from supernovae and AGN, etc.). New observational techniques and improved instrumentations allow us to look back further in time and study the cosmic evolution of galaxies. However, to understand the observations and thus the evolution of galaxies, we need to combine numerical simulations and semi-analytical models with the observations.

Semi-analytical models of galaxy formation and evolution can be used to interpret the observations and give predictions within the framework of the hierarchical evolution of dark matter haloes, without the resolution limitation of numerical simulations. These models use simple, analytic models to calculate the evolution of the baryonic component and generate merger trees to trace the hierarchical structure formation (e.g. Cole et al. 2000a; Baugh 2006). Semi-analytical models are flexible, many process can be modelled together and a wide range of galaxy properties can be calculated. The main limitations of semi-analytical models are the need for simplifying assumptions (e.g spherical symmetry) and that some processes are modelled in a deterministic way (e.g. supernova feedback). However, as we learn more about the details of each process that plays an important role in the evolution of galaxies, the models can be improved and the paramateres can be updated.

In the appended paper we present simulation results performed by a new development of the GALFORM semi-analytical cosmological model, developed mainly at Durham University, implemented in a new Millenium Simulation run with *WMAP7* cosmology (Cole et al. 2000b; Komatsu et al. 2011; Lagos et al. 2012; Gonzalez-Perez et al. 2014). GALFORM models all the important processes that determine the formation and evolution of galaxies, including the collapse and merging of dark matter haloes; gas heating and cooling through shocks and radiative cooling inside dark matter haloes, leading to the formation of galactic disks; star formation; feedback from supernovae, AGN and from the photoionization of the IGM; chemical enrichment of gas and stars; galaxy mergers leading to the formation of stellar spheroids and collapse of gravitationally unstable disks. The galaxy luminosities are determined by combining the star formation and metal enrichment histories with SPS models for each galaxy. The attenuation of starlight by dust is included based on radiative transfer canculations. The model also includes a sophisticated model of black hole growth and AGN feedback. The final output of the simualtion is a prediction of the number and properties of galaxies that reside within the dark matter haloes of different masses. The detailed description of GALFORM can be found in Fanidakis et al. (2011, 2012); Lagos et al. (2012); Gonzalez-Perez et al. (2014)
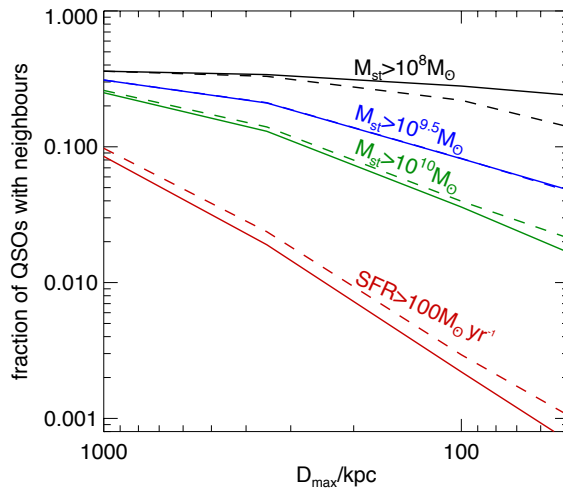
Figure 4.2: Fraction of QSOs with neighbours as a function of the aperture used for the search. The black, blue and green lines show this fraction in case of neighbours with different stellar masses ($M_\star > 10^8\,\mathrm{M_\odot}$, $> 10^{9.5}\,\mathrm{M_\odot}$, $> 10^{10}\,\mathrm{M_\odot}$, respectively), while the red lines represent the fraction of QSOs with bright neighbours (SFR > 100 $\mathrm{M_\odot\,yr^{-1}}$) as a function of aperture, in case of the Gonzalez-Perez14 (solid lines) and Gonzalez-Perez14.GRP (dashed lines) models

4.3 Summary of the appended paper

With the aim of investigating the properties of the companion galaxy of SMM J04135+10277, we use archive optical (*HST* WFPC2, CFHT MegaPrime/MegaCam) and infrared (*Spitzer* IRAC and MIPS, SCUBA) data and new APEX ArTeMiS $350\,\mu$m observations to construct its spectral energy distribution (Figure 4.1). The companion galaxy is not seen in the optical bands, hence it was missed during the original identifications (Knudsen et al. 2003). To model the SED we use the starburst SED model of Groves et al. (2008) and the SED fitting code MAGPHYS (da Cunha et al. 2008, 2015). Based on the SED modelling the companion galaxy of SMM J04135+10277 is a heavily dust obscured ($A_\mathrm{V} \gtrsim 2.8\,\mathrm{mag}$), star-forming galaxy with a star formation rate of $\sim 1000\,\mathrm{M_\odot\,yr^{-1}}$.

As in most quasar–star-forming galaxy systems, the host galaxy of the quasar is also gas-rich, our main question is whether the case of SMM J04135+10277 is unique or common at high-z. In order to investigate the expected frequency of such systems, we use the cosmological semi-analytic model, GALFORM (Gonzalez-Perez et al. 2014). We take the outputs of the simulation at $z = 2.8$ to find quasar–companion pairs at different separations. We find that 22% of our simulated quasar sample have at least one companion galaxy in their $< 100\,\mathrm{kpc}$ environment and 0.3% have bright, star-forming companions (SFR $> 100\,\mathrm{M_\odot\,yr^{-1}}$; Figure 4.2).

To make a direct comparison between the model predictions and the case of SMM J04135+10277, we focus on systems with an integrated SFR of $> 500 \, \mathrm{M_\odot \, yr^{-1}}$ inside the aperture and compute their relative gas content and SFR. We find that in 67% of these systems the molecular gas mass of the quasars' host galaxies is lower compared to the integrated value of their companion at a distance of $< 50 \, \mathrm{kpc}$ and the star formation is dominated by the companion galaxies and not the quasars' hosts. This means that the case of SMM J04135+10277 is representative of highly star-forming quasar–companion galaxy systems at $z = 2.8$. In the discussion section we compare our findings with observations of high-redshift quasars and HzRGs found in the literature.

Chapter 5

Outlook and future prospects

Studies of high-z quasars and HzRGs and their environment indicate that these AGN might be signposts of overdense regions in the Universe, surrounded by submm galaxies and often associated with close gas-rich, star-forming companions. These results demonstrate that we are on the right track to understand the evolution of massive, elliptical galaxies. However, the biggest limiting factor of high-z studies is angular resolution. To date, far-infared surveys of quasars have been perfomed with e.g. the *Herschel Space Observatory* or SCUBA(-2) at the JCMT but these observations do not provide sufficient spatial resolution to resolve FIR emission and to pinpoint its exact origin (e.g. SCUBA beam is 15" at 850 μm, *Herschel* SPIRE beam at 250 μm is $\sim$ 18"). These surveys revealed several quasars with very high FIR luminosities indicating high SFR in their host galaxies. The question is whether they are indeed going through a starburst and reaching their maximum SFR or the FIR emission comes from multiple galaxies blended in a large beam. Both scenarios are possible: e.g. Wang et al. (2013) measured the dust continuum of $z = 6$ quasars with ALMA and their measurements indicate vigorous star formation over the central region in the quasar host galaxies, while Emonts et al. (2015) concluded that one the most IR luminous HzRG MRC0152-209 is in fact a triple merger system and the high IR emission is the result of intense star formation in each galaxy component.

The strength of submm interferometers has been demonstrated in case of high-z submm galaxies (SMGs), where a fraction of SMGs resolved into multiple distinct sources compared to large beam observations (e.g. Wang et al. 2011; Smolčić et al. 2012; Barger et al. 2012; Hodge et al. 2013; Karim et al. 2013). Therefore, it is possible that *Herschel* detected FIR-bright quasars might have unresolved companion galaxies and thus the use of high resolution observations is essential.

In addition to submm studies, we can use other tracers to characterise the environment of high-z AGN, such as CO transition lines to determine the properties of the molecular gas (physical conditions, mass), and for kinematic studies or the

optically thin CII cooling line, which can be used to estimate SFR, even in case of obscured galaxies.

To continue our work, we found a potential AGN–gas-rich companion galaxy candidate, the HzRG TXS0828+193 ($z = 2.6$). This radio galaxy is associated with a luminous CO(3-2) line emission detected by the IRAM PdBI (Nesvadba et al. 2009). The CO(3-2) emission-line region is located $\sim$10" (80 kpc) south-west from the radio galaxy and it is aligned with the axis of the radio jet. The integrated CO spectrum shows two compact components, both of them have the same spatial position but different velocity offsets. The total molecular gas mass of the two components is $M_{H_2} \sim 1.4 \times 10^{10}\,M_\odot$. The CO emission region does not have a counterpart within the 5" beam in the *Spitzer* IRAC and MIPS 24 μm bands, nor in the optical, making this case more challenging than that of SMM J04135. Nesvadba et al. (2009) proposed two possible scenarios for the origin of the CO emission. The CO source might be an extremely gas-rich satellite galaxy with a stellar mass of $< 3 \times 10^9\,M_\odot$, which is in a very young stage of the starburst, hence the non-detection in the mid-IR bands. Such satellite galaxy has been found close to the HzRG 4C60.07, indicating an early-stage merger of the young radio galaxy and a gas-rich starburst/AGN (Ivison et al. 2008).

The second alternative suggests, that the CO emission comes from a cold cloud or filament in the halo of the radio galaxy. Such filaments have been found in some low-z cooling-flow clusters and also in the Perseus cluster, where some of the low temperature, higher density ambient medium is carried by the radio jet-driven outward moving bubbles, leading to runaway cooling instabilities, that generate filamentary structures at greater radii (Salomé et al. 2008). The only way to distinguish between these two scenarios is to use high resolution CO and submillimeter observations.

To investigate the origin of the CO emission in the HzRG TXS0828+193 and to continue the study of the system of SMM J04135+10277, we had proposed for ALMA submm and CO line observations (Cycle 3). Our project is approved and we are waiting for the data delivery.

Bibliography

Aalto, S., Garcia-Burillo, S., Muller, S., et al. 2012, A&A, 537, A44

Aird, J., Nandra, K., Laird, E. S., et al. 2010, MNRAS, 401, 2531

Antonucci, R. 1993, ARA&A, 31, 473

Barger, A. J., Wang, W.-H., Cowie, L. L., et al. 2012, ApJ, 761, 89

Barthel, P. D. 1989, ApJ, 336, 606

Baugh, C. M. 2006, Reports on Progress in Physics, 69, 3101

Blain, A. W., Smail, I., Ivison, R. J., Kneib, J.-P., & Frayer, D. T. 2002, Phys. Rep., 369, 111

Boehringer, H., Voges, W., Fabian, A. C., Edge, A. C., & Neumann, D. M. 1993, MNRAS, 264, L25

Bouwens, R. J., Illingworth, G. D., Franx, M., & Ford, H. 2007, ApJ, 670, 928

Bruzual, G. & Charlot, S. 2003, MNRAS, 344, 1000

Casey, C. M., Narayanan, D., & Cooray, A. 2014, Phys. Rep., 541, 45

Chabrier, G. 2003, PASP, 115, 763

Charlot, S. & Fall, S. M. 2000, ApJ, 539, 718

Clements, D. L., Petitpas, G., Farrah, D., et al. 2009, ApJ, 698, L188

Cole, S., Benson, A., Baugh, C., Lacey, C., & Frenk, C. 2000a, in Astronomical Society of the Pacific Conference Series, Vol. 200, Clustering at High Redshift, ed. A. Mazure, O. Le Fèvre, & V. Le Brun, 109

Cole, S., Lacey, C. G., Baugh, C. M., & Frenk, C. S. 2000b, MNRAS, 319, 168

Conroy, C. 2013, ARA&A, 51, 393

Croft, S., Kurk, J., van Breugel, W., et al. 2005, AJ, 130, 867

da Cunha, E., Charlot, S., & Elbaz, D. 2008, MNRAS, 388, 1595

da Cunha, E., Walter, F., Smail, I. R., et al. 2015, ApJ, 806, 110

Daddi, E., Cimatti, A., Renzini, A., et al. 2004, ApJ, 617, 746

De Breuck, C., Downes, D., Neri, R., et al. 2005, A&A, 430, L1

Dekel, A., Birnboim, Y., Engel, G., et al. 2009, Nature, 457, 451

Dunn, R. J. H. & Fabian, A. C. 2006, MNRAS, 373, 959

Dunn, R. J. H. & Fabian, A. C. 2008, MNRAS, 385, 757

Eckart, A. & Genzel, R. 1996, Nature, 383, 415

Elston, R., Rieke, G. H., & Rieke, M. J. 1988, ApJ, 331, L77

Emonts, B. H. C., De Breuck, C., Lehnert, M. D., et al. 2015, A&A, 584, A99

Fabian, A. C. 2012, ARA&A, 50, 455

Fall, S. M. & Efstathiou, G. 1980, MNRAS, 193, 189

Fanaroff, B. L. & Riley, J. M. 1974, MNRAS, 167, 31P

Fanidakis, N., Baugh, C. M., Benson, A. J., et al. 2011, MNRAS, 410, 53

Fanidakis, N., Baugh, C. M., Benson, A. J., et al. 2012, MNRAS, 419, 2797

Feruglio, C., Maiolino, R., Piconcelli, E., et al. 2010, A&A, 518, L155

Fischera, J. & Dopita, M. 2005, ApJ, 619, 340

Fischera, J. & Dopita, M. A. 2004, ApJ, 611, 919

Franx, M., Labbé, I., Rudnick, G., et al. 2003, ApJ, 587, L79

Gebhardt, K., Bender, R., Bower, G., et al. 2000, ApJ, 539, L13

Genzel, R., Pichon, C., Eckart, A., Gerhard, O. E., & Ott, T. 2000, MNRAS, 317, 348

Ghez, A. M., Klein, B. L., Morris, M., & Becklin, E. E. 1998, ApJ, 509, 678

Gonzalez-Perez, V., Lacey, C. G., Baugh, C. M., et al. 2014, MNRAS, 439, 264

Greene, J. E., Zakamska, N. L., & Smith, P. S. 2012, ApJ, 746, 86

Greve, T. R., Stern, D., Ivison, R. J., et al. 2007, MNRAS, 382, 48

Groves, B., Dopita, M. A., Sutherland, R. S., et al. 2008, ApJS, 176, 438

Gullberg, B., De Breuck, C., Lehnert, M. D., et al. 2016, A&A, 586, A124

Heckman, T. M. & Best, P. N. 2014, ARA&A, 52, 589

Hodge, J. A., Karim, A., Smail, I., et al. 2013, ApJ, 768, 91

Hopkins, A. M. 2004, ApJ, 615, 209

Hopkins, P. F., Hernquist, L., Cox, T. J., et al. 2006, ApJS, 163, 1

Hopkins, P. F., Hernquist, L., Cox, T. J., & Kereš, D. 2008, ApJS, 175, 356

Husband, K., Bremer, M. N., Stanway, E. R., & Lehnert, M. D. 2015, MNRAS, 452, 2388

Ivison, R. J., Dunlop, J. S., Smail, I., et al. 2000, ApJ, 542, 27

Ivison, R. J., Morrison, G. E., Biggs, A. D., et al. 2008, MNRAS, 390, 1117

Ivison, R. J., Smail, I., Amblard, A., et al. 2012, MNRAS, 425, 1320

Jones, S. F., Blain, A. W., Lonsdale, C., et al. 2015, MNRAS, 448, 3325

Karim, A., Swinbank, A. M., Hodge, J. A., et al. 2013, MNRAS, 432, 2

Katz, N., Keres, D., Dave, R., & Weinberg, D. H. 2003, in Astrophysics and Space Science Library, Vol. 281, The IGM/Galaxy Connection. The Distribution of Baryons at z=0, ed. J. L. Rosenberg & M. E. Putman, 185

Kereš, D., Katz, N., Weinberg, D. H., & Davé, R. 2005, MNRAS, 363, 2

Knudsen, K. K., van der Werf, P. P., & Jaffe, W. 2003, A&A, 411, 343

Komatsu, E., Smith, K. M., Dunkley, J., et al. 2011, ApJS, 192, 18

Kormendy, J. & Ho, L. C. 2013, ARA&A, 51, 511

Kormendy, J. & Richstone, D. 1995, ARA&A, 33, 581

Kroupa, P. 2002, Science, 295, 82

Kurk, J. D., Pentericci, L., Overzier, R. A., Röttgering, H. J. A., & Miley, G. K. 2004a, A&A, 428, 817

Kurk, J. D., Pentericci, L., Röttgering, H. J. A., & Miley, G. K. 2004b, A&A, 428, 793

Kurk, J. D., Röttgering, H. J. A., Pentericci, L., et al. 2000, A&A, 358, L1

Lagos, C. d. P., Bayet, E., Baugh, C. M., et al. 2012, MNRAS, 426, 2142

Lanz, L., Zezas, A., Brassington, N., et al. 2013, ApJ, 768, 90

Leitherer, C., Schaerer, D., Goldader, J. D., et al. 1999, ApJS, 123, 3

Madau, P. & Dickinson, M. 2014, ARA&A, 52, 415

Magorrian, J., Tremaine, S., Richstone, D., et al. 1998, AJ, 115, 2285

Marconi, A. & Hunt, L. K. 2003, ApJ, 589, L21

McNamara, B. R., Wise, M., Nulsen, P. E. J., et al. 2000, ApJ, 534, L135

Merritt, D. & Ferrarese, L. 2001, MNRAS, 320, L30

Morganti, R., Holt, J., Saripalli, L., Oosterloo, T. A., & Tadhunter, C. N. 2007, A&A, 476, 735

Nesvadba, N. P. H., Neri, R., De Breuck, C., et al. 2009, MNRAS, 395, L16

Nesvadba, N. P. H., Polletta, M., Lehnert, M. D., et al. 2011, MNRAS, 415, 2359

Netzer, H. 2015, ARA&A, 53, 365

Partridge, R. B. & Peebles, P. J. E. 1967, ApJ, 147, 868

Pentericci, L., Kurk, J. D., Röttgering, H. J. A., et al. 2000, A&A, 361, L25

Priddey, R. S., Ivison, R. J., & Isaak, K. G. 2008, MNRAS, 383, 289

Prochaska, J. X. & Hennawi, J. F. 2009, ApJ, 690, 1558

Rees, M. J. & Ostriker, J. P. 1977, MNRAS, 179, 541

Richstone, D., Ajhar, E. A., Bender, R., et al. 1998, Nature, 395, A14

Riechers, D. A. 2013, ApJ, 765, L31

Riechers, D. A., Walter, F., Carilli, C. L., Bertoldi, F., & Momjian, E. 2008, ApJ, 686, L9

Rowlands, K., Dunne, L., Dye, S., et al. 2014, MNRAS, 441, 1017

Rupke, D. S. N. & Veilleux, S. 2013, ApJ, 775, L15

Salomé, P., Combes, F., Revaz, Y., et al. 2008, A&A, 484, 317

Salomé, P., Guélin, M., Downes, D., et al. 2012, A&A, 545, A57

Salpeter, E. E. 1955, ApJ, 121, 161

Sanders, D. B. & Mirabel, I. F. 1996, ARA&A, 34, 749

Silk, J. 1977, ApJ, 211, 638

Silva, A., Sajina, A., Lonsdale, C., & Lacy, M. 2015, ApJ, 806, L25

Smolčić, V., Aravena, M., Navarrete, F., et al. 2012, A&A, 548, A4

Smolčić, V., Karim, A., Miettinen, O., et al. 2015, A&A, 576, A127

Springel, V., White, S. D. M., Jenkins, A., et al. 2005, Nature, 435, 629

Steidel, C. C., Pettini, M., & Hamilton, D. 1995, AJ, 110, 2519

Stevens, J. A., Ivison, R. J., Dunlop, J. S., et al. 2003, Nature, 425, 264

Stevens, J. A., Jarvis, M. J., Coppin, K. E. K., et al. 2010, MNRAS, 405, 2623

Stevens, J. A., Page, M. J., Ivison, R. J., Smail, I., & Carrera, F. J. 2004, ApJ, 604, L17

Tadhunter, C. 2008, New A Rev., 52, 227

Urry, C. M. & Padovani, P. 1995, PASP, 107, 803

van de Voort, F., Schaye, J., Booth, C. M., & Dalla Vecchia, C. 2011a, MNRAS, 415, 2782

van de Voort, F., Schaye, J., Booth, C. M., Haas, M. R., & Dalla Vecchia, C. 2011b, MNRAS, 414, 2458

Venemans, B. P., Röttgering, H. J. A., Miley, G. K., et al. 2007, A&A, 461, 823

Vogelsberger, M., Genel, S., Springel, V., et al. 2014, Nature, 509, 177

Walter, F., Weiss, A., & Scoville, N. 2002, ApJ, 580, L21

Wang, R., Wagg, J., Carilli, C. L., et al. 2013, ApJ, 773, 44

Wang, W.-H., Cowie, L. L., Barger, A. J., & Williams, J. P. 2011, ApJ, 726, L18

White, S. D. M. & Frenk, C. S. 1991, ApJ, 379, 52

Wylezalek, D., Galametz, A., Stern, D., et al. 2013, ApJ, 769, 79